Title

The Development of Steady-State Activation Hubs between Adult LTi ILC3s and Primed Macrophages in Small Intestine

Journal

The Journal of Immunology, 199(5)

ISSN

0022-1767

Authors

Savage, Adam K

Liang, Hong-Erh

Locksley, Richard M

Publication Date

2017-09-01

DOI

10.4049/jimmunol.1700155

Peer reviewed

HHS Public Access

Author manuscript

J Immunol. Author manuscript; available in PMC 2018 September 01.

Published in final edited form as:

J Immunol. 2017 September 01; 199(5): 1912–1922. doi:10.4049/jimmunol.1700155.

The development of steady-state activation hubs between adult LTi ILC3s and primed macrophages in small intestine

Adam K. Savage[*], **Hong-Erh Liang**[†], and **Richard M. Locksley**[*,†,‡,1]

[*]Howard Hughes Medical Institute, University of California, San Francisco, San Francisco, California, USA

[†]Department of Medicine, University of California, San Francisco, San Francisco, California, USA

[‡]UCSF Helen Diller Family Comprehensive Cancer Center, University of California, San Francisco, San Francisco, California, USA

Abstract

Group 3 innate lymphoid cells (ILC3s) are important for intestinal health, particularly in controlling inflammation in response to epithelial dysregulation, but their role during homeostasis remains less well understood. We generated IL-22 reporter mice to assess production of this key cytokine by ILC3s in the small intestine during development and under basal conditions. Although IL-22 is produced by a variety of lymphocyte populations, constitutively high IL-22 expression was limited to lymphoid-tissue inducer (LTi) cells residing in lymph node-like structures in the gut called small intestinal lymphoid tissues (SILT). Constitutive IL-22 expression was dependent on the microbiota and MyD88 signaling, appeared upon weaning, and was present across the spectrum of SILT, including in cryptopatches. Activated SILT LTi cells colocalized with a rare subpopulation of activated macrophages constitutively positive for IL-12/23 p40 and capable of activating neonatal LTi cells in response to TLR stimulus. Thus, weaning leads to the organization of innate immune activation hubs at SILT that mature and are continuously sustained by signals from the microbiota. This functional and anatomic organization constitutes a significant portion of the steady-state IL-23/IL-22 axis.

INTRODUCTION

The intestinal immune system constitutes a diverse assemblage of cells reflecting the challenge of discriminatory responses to the abundant microbiota and fluctuating microbial and metabolic stimuli. The single-cell-thick epithelia maintaining this barrier are key targets of IL-22, an epithelial growth factor produced by intestinal lymphocytes (1). Many intestinal lymphocytes produce IL-22, including αβ T cells, γδ T cells, and two types of *Rorc*-dependent group 3 innate lymphoid cells (ILC3s): NKp46^{+} ILC3s and NKp46^{-} ILC3s, including lymphoid-tissue inducer cells and adult LTi-like cells (LTi cells). Likewise, a variety of stimuli can induce IL-22 production from these cells, including IL-23, IL-1β,

AUTHOR CORRESPONDENCE: Richard M. Locksley, 513 Parnassus Ave, S1032B, San Francisco, CA 94143-0795, richard.locksley@ucsf.edu, Tel: (415) 476-1559, Fax: (415) 502-5081.

[1]This work was supported by the National Institutes of Health grants AI30663 and HL128903 and the Howard Hughes Medical Institute (HHMI). A.K.S. is an HHMI fellow.

IL-6, lymphotoxin, and aryl hydrocarbon receptor ligands. The breadth of this system reflects the integral role of IL-22 as a mediator of intestinal barrier function and homeostasis.

The role of IL-22 in intestinal health has been well-described in the context of epithelial disruption, as occurs during *Citrobacter rodentium* infection (2–4) and dextran sulfate sodium-induced colitis (5, 6). These systems helped to establish that lymphocytes capable of IL-22 production are dispersed throughout the intestinal lamina propria, presumably within functional distance from target IL-22 receptor-expressing epithelial cells, intermingled with myeloid cells capable of inducing IL-22 (7). How and where IL-22 acts during homeostasis is less evident, although homeostatic function is suggested by impaired anti-microbial defense (8) and dysbiosis (9) that occurs in the absence of this cytokine or when upstream regulators are perturbed (10–13).

However, one of the primary sources of IL-22 is LTi cells which are preferentially clustered in anatomically distinct aggregates known as solitary intestinal lymphoid tissue (SILT) (14, 15). There are hundreds to thousands of SILT aggregates in mouse small intestine which comprise a continuum from nascent to fully developed B cell follicles, designated cryptopatches (CPs) and isolated lymphoid follicles (ILFs), respectively (16). Though existing within the submucosa of the lamina propria, these structures are akin to lymph nodes and are dependent on many of the same factors. While CPs develop independently of the microbiota (17), their progeny ILFs require microbial sensing pathways (18, 19), suggesting that CPs are quiescent structures which develop into ILFs in response to microbial signals derived from the intestinal lumen. $CD11c^+$ APCs residing in CP are likely responsible, at least in part, for this sensing capability. However, little is known about how SILT-resident APCs relate to or can be distinguished from the dense network of related cells blanketing the lamina propria.

Genetic models utilizing CD11c (10, 11) and CX3CR1 (12, 13) alleles have established a role for intestinal monocytes in IL-22 biology and provide evidence for dysbiosis and tissue alterations under steady-state conditions. This highlights the possibility that the effects of IL-22 in models of inflammation may also integrate its effects on baseline tissue homeostasis. This cryptic inflammation reveals that continuous immune surveillance of the microbiota is likely necessary to sustain epithelial health and supports a homeostatic role for IL-22 in these basal functions (20, 21). CD11c and CX3CR1, however, are broadly expressed by intestinal monocytes, including both macrophages and dendritic cells (DCs) (22), and therefore do not provide anatomic resolution as to if and where these pathways are active in the intestinal landscape.

In order to better understand the functional and anatomic axis in steady-state mouse intestine, we leveraged sensitive cytokine reporter mice to assay the localization and activation of critical cellular components of the IL-22 pathway. A unique *Il22* reporter mouse revealed intense induction of IL-22 in SILT-localized LTi cells upon weaning. Also present at SILT were a subset of macrophages displaying heightened activation typified by induction of the IL-12 and IL-23 subunit IL-12/23 p40. Activity of these macrophages could be regulated by CpG and CpG was capable of precociously inducing activation of LTi cells

in neonatal mice. These data demonstrate that SILT are activated earlier than previously recognized and constitute a localizing site for IL-23-producing intestinal macrophages.

METHODS

Il22 reporter mice

Il22 reporter/knockout mice (Catch22) were generated by homologous gene targeting in C57BL/6 embryonic stem cells. The previously published plasmid pKO915-DT (Lexicon) was modified to express tdTomato in place of YFP, such that the cassette now contained (in order from 5′ to 3′) genomic sequence of the rabbit β-globin gene partial exon 2–3, the gene encoding tdTomato (Clontech), encephalomyocarditis virus IRES, humanized Cre recombinase, bovine growth hormone poly(A) tail, and a *lox*P-flanked neomycin resistance cassette. ~3 kilobase homologous arms straddling the *Il22* translation initiation site were amplified from C57BL/6 genomic DNA using Phusion polymerase (Finnzymes) and cloned into the cassette by standard methods. The construct was linearized with NotI and transfected by electroporation into C57BL/6 embryonic stem cells. Cells were grown on irradiated feeders with the aminoglycoside G418 in the media, and resistant clones were screened for 5′ and 3′ homologous recombination by PCR. Six clones were confirmed by PCR and two were selected for injection into albino C57BL/6 blastocysts to generate chimeras. The male chimeric pups with highest ratios of black-to-white coat color from each clone were selected to breed with homozygous CMV-Cre transgenic C57BL/6 females (B6.C-Tg(CMV-cre)1Cgn/J; 006054, obtained from The Jackson Laboratory) to excise the neomycin resistance cassette and subsequently to wild-type C57BL/6 to remove the CMV-Cre allele. Initial phenotyping of both clones did not reveal differences and one was selected for subsequent experiments. In most cases reporter heterozygous or homozygous males were bred to reporter heterozygous or C57BL/6 female mice, such that the dam was IL-22 sufficient whenever possible.

Other mice

C57BL/6J (000664), Yet40 (B6.129-*Il12b*^{tm1Lky}/J; 006412), CD11c-Cre (B6.Cg-Tg(Itgax-cre)1-1Reiz/J; 008068), Villin-Cre (B6.Cg-Tg(Vil1-cre)997Gum/J; 004586), MyD88-flox (B6.129P2(SJL)-*Myd88*^{tm1Defr}/J; 008888), Rosa-DTα (B6.129P2-*Gt(ROSA)26Sor*$^{tm1(DTA)Lky}$/J; 009669), RORγt-GFP (B6.129P2(Cg)-*Rorc*^{tm2Litt}/J; 007572), IL-1 receptor knockout (B6.129S7-*Il1r1*^{tm1Imx}/J; 003245), and IL-18 receptor knockout (B6.129P2-*Il18r1*^{tm1Aki}/J; 004131) mice were from The Jackson Laboratory. All mice were maintained on standard chow and water, except for antibiotic-treatment experiments in which they were maintained on Ampicillin, Metronidazole, Neomycin (1 mg/ml each), and Vancomycin (0.5 mg/ml) in 1% sucrose, from approximately embryonic day 14 to four weeks of age. All mice were made using C57BL/6 ES cells or backcrossed at least 10 generations onto the C57BL/6 background and were maintained according to institutional guidelines in specific pathogen-free facilities at the University of California, San Francisco (San Francisco, CA).

Cell isolation and flow cytometry

For isolation of intestinal lamina propria for flow cytometry the small intestine, large intestine, and cecum were dissected separately, flushed extensively with cold PBS, and the mesenteric tissue was removed. Peyer's patches and cecal patches were removed and in some cases processed and analyzed separately. Lymphoid structures were not removed from the large intestine lamina propria. The intestinal pieces were turned inside-out and shaken in four changes of 20 ml cold PBS and washed for 20 minutes at 37°C in two changes of 20 ml Ca^{2+}/Mg^{2+} free HBSS containing 5 mM DTT; 5 mM EDTA; 10 mM HEPES; 2% FCS, followed by 20 ml of Ca^{2+}/Mg^{2+} replete HBSS containing 10 mM HEPES; 2% FCS. Tissues were digested for 30 minutes at 37°C in 5 ml Ca^{2+}/Mg^{2+} replete HBSS containing 10 mM HEPES; 2% FCS; 30 μg/ml DNaseI (Roche); 0.1 Wünsch/ml LibTM (Roche), and homogenized in C tubes using a gentleMACS tissue dissociator (Miltenyi). Homogenate was passed through a 100 μm filter, separated on a 40%/90% Percoll gradient, and enumerated for staining equivalent numbers for flow cytometry. For analysis of the epithelial fraction, supernatant from the washes was saved, combined, filtered and separated on a Percoll gradient as above, without digest. For isolation of punch biopsies, tissue was fileted and washed as above. Tissue was laid open in a petri dish, periodically bathed with cold PBS and observed under low power with dsRed excitation using a Leica DM IL LED microscope with fluorescent illumination. SILT of approximately one villus width or less were isolated using a 0.5 mm punch biopsy tool and digested as above. For staining of intracellular IL-22, lamina propria preps were performed as above with the inclusion of 0.5 mg/ml Brefeldin A (BioLegend) in all buffers until fixation for intracellular staining by standard procedures. The following antibodies (from BioLegend, eBioscience, Becton Dickinson) were used for staining: CCR6 (29-2L17), CD3 (17A2), CD4 (RM4-5), CD11b (M1/70), CD11c (N418), CD45 (30-F11), CD64 (X54-5/7.1), CD69 (H1.2F3), CD90.2 (Thy1; 53-2.1), CD103 (M290), CD172a (P84), ckit (ACK2), F4/80 (BM8), γδTCR (GL3), IL-22 (IL22JOP), Ly6C (RB6-8C5), MerTK (DS5MMER), MHCII (M5/114.15.2), NKp46 (29A1.4), TCRβ (H57), TLR3 (11F8), TLR9 (M9.D6). Data were acquired with a Becton Dickinson LSRII or Fortessa and analyzed using FlowJo (Tree Star). Cell sorting was performed with a Beckman Coulter MoFlo XDP. Gating examples are provided in Supplementary Figure 1B and Supplementary Figure 4E–F.

Immunofluorescence

For analysis by immunofluorescence, tissues were harvested, flushed extensively with cold PBS, and fileted. For whole mount, fileted intestine was washed with DTT/EDTA and rinsed in HBSS, as for flow cytometry above. Intestinal pieces were laid flat between Whatman paper with light pressure for 4 hours in 2% paraformaldehyde with 2 mM $MgCl_2$ and 1.25 mM EGTA at 4°C, then washed overnight in excess PBS. For thin section, the tissue was also dehydrated in 30% sucrose for >4 hours before rolling the tissue on a wooden stick, mounting in OCT as a 'swiss roll', and cutting 8 um sections with a cryostat. Thin sections were stained and mounted per standard procedures. Tissue for whole mount was stained in 0.5% TritonX-100 per standard procedures. Images were acquired and processed with a Zeiss Axio Imager 2 and Adobe Photoshop.

Quantitative PCR

For transcript analysis of 0.5 mm washed ileum or small intestine punches, tissue was homogenized in 1 ml buffer RLT (Qiagen) in M tubes using a gentleMACS tissue dissociator and spun through a QiaShredder tube (Qiagen) prior to freezing at −80°C. Sorted cells were pelleted and frozen in buffer RLT. RNA was made from cell homogenate with the RNeasy Mini or Micro kit (Qiagen) and immediately transcribed into cDNA using Superscript III Reverse Transcriptase (Invitrogen). Quantitative PCR was performed using Power SYBR Green (Invitrogen) on an Applied Biosystems StepOnePlus and analyzed using Microsoft Excel. Primers were constructed from the Ensembl mouse (C57BL/6) genome database using Primer3Plus (http://primer3plus.com/cgi-bin/dev/primer3plus.cgi). The primers used were:

18s (GAAACGGCTACCACATCCAAG, TTACAGGGCCTCGAAAGAGTC),

Batf3 (ACCCAGAAGGCTGACAAGC, TCCTCCTTCAGCTTCGAAATC),

Il1b (GGACCCATATGAGCTGAAAGC, TTGTCGTTGCTTGGTTCTCC),

Il6 (ACAAAGCCAGAGTCCTTCAGAG, TGGAAATTGGGGTAGGAAGG),

Il10 (GAATTCCCTGGGTGAGAAGC, AATCACTCTTCACCTGCTCCAC),

Il12a (AACCTGCTGAAGACCACAGATG, GTTTGGTCCCGTGTGATGTC),

Il12b (CATCTGCTGCTCCACAAGAAG, GGTGCTTCACACTTCAGGAAAG),

Il17a (AAGGCCCTCAGACTACCTCAAC, TGAGCTTCCCAGATCACAGAG),

Il22 (AATCGCCTTGATCTCTCCAC, TTCTGGATGTTCTGGTCGTC),

Il22ra2 (AAGCATTGCCTTCTAGGTCTC, TGGACTGAAATCGGACCTTC),

Il23a (CATGGAGCAACTTCACACCTC, TAGAACTCAGGCTGGGCATC),

Irak3 (AGGAATAGCCAAAGCCATCC, GTTGGAGCTGGTCATCCAAG),

Klf4 (TCTCATCTCAAGGCACACCTG, TAGTGCCTGGTCAGTTCATCG),

Lta (ACCCATGGCATCCTGAAAC, GAGAAGCCATGTCGGAGAAAG),

Ltb (GCAGTGCCTATCACTGTCCTG, TTTCTGAGCCTGTGCTCCTG),

Tnfa (CTCTTCTCATTCCTGCTTGTGG, ATGAGAGGGAGGCCATTTG),

Wfdc18 (TACTGCCTGGGCTCTGTCTAAC, TCCTGTGCATCGTTCATCAC),

Zbtb46 (GGTGATGATGGCTCACTTCTG, GGGCACTTGAACTTCTTCCTG).

Macrophage cultures and protein detection

For analysis of cytokine potential, intestinal macrophages were sorted and pooled from 5–6 *Il12b*$^{Y40/Y40}$ mice and cultured at 18,000 cells per well of a non-treated U-bottom 96-well plate for 18–21 hours. Culture medium was RPMI with 10% FCS, supplemented with 10 ng/ml GM-CSF (R&D Systems) with or without 2 μg/ml each LMW and HMW poly(I:C) or 5 μM CpG (ODN1826) (Invivogen). Culture supernatants were harvested, stored at −80°C and analyzed for cytokine production by Cytometric Bead Array (Becton Dickinson).

Neonatal treatments

For activation of neonatal LTi cells *in vivo*, 12–14 day-old *Il22*$^{C22/+}$;*Il12b*$^{Y40/Y40}$ mice were injected i.p. with either PBS, 2.5 μg IL-23 (R&D Systems), 100 μg CpG (ODN1826), or 100 μg poly(I:C) (Invivogen) in 50 μl on 2 consecutive days for analysis on the third day.

Graphing and statistical analysis

Charts and statistical analysis was performed using Prism (GraphPad). Where applicable, significance was determined using unpaired t tests with Holm-Sidak correction for multiple comparisons with an alpha of 0.05. Otherwise single t tests were used with the P value indicated in the figure legend.

RESULTS

Il22 is constitutively active in healthy mouse intestine

To assess the sources of IL-22 in healthy intestine, we generated a tdTomato-Cre knock-in/knock-out allele at the *Il22* locus in C57BL/6 mice (Supplementary Figure 1A) termed 'Catch22' ('C22'; Cre-Associated Transcript CHasing IL-22). Previous publications using other *Il22* reporter mice did not assess the anatomic distribution of *Il22*$^{+}$ cells in healthy small intestine (23, 24). Therefore, we first determined Catch22 fluorescence by whole-mount staining and found cells expressing the reporter allele were present in discrete clusters throughout the small intestine, as assessed using native fluorescence (data not shown) or by antibody staining for the tdTomato protein (Figure 1A–C). These clusters were SILT based upon their number and distribution, their colocalization with CD11c^{+} and VCAM1^{+} cells(25) after immunostaining (Figure 1D), and their colocalization in larger clusters with B220^{+} B cells. Longer exposure times revealed cells more dim for tdTomato signal scattered throughout the lamina propria without a discernable spatial arrangement (data not shown).

We focused on the SILT-resident cells as they were the brightest and could be identified in flow cytometry by high levels of Catch22 signal. Flow cytometry of small intestine from 6 week-old *Il22*$^{C22/+}$ mice revealed IL-22 was produced by Thy1^{+} cells, including CD4^{+} αβ T cells, γδ T cells, and ILCs (Thy1^{+} CD3^{-}) (Figure 1E and Supplementary Figure 2A), as previously reported (23, 24). At steady-state, the absolute number of Catch22^{+} ILCs vastly outnumbered Catch22^{+} T cells. Among the ILC populations, a larger number of NKp46^{-} ckit^{hi} than NKp46^{+} ILCs constitutively expressed the Catch22 allele, even though the total number of these two cell types was comparable (Supplementary Figure 2B–D).

In accordance with the immunofluorescence data, we found that Catch22 MFI distinguishes the major ILC3 subtypes. Catch22^{hi} ILCs in the steady-state intestine were almost entirely of the LTi cell phenotype, as defined by their CD3^{-}, ckit^{hi}, NKp46^{lo} (Figure 1E and Supplementary Figure 2E), and CCR6^{hi} phenotype (Supplementary Figure 2F), and abundant transcripts for lymphotoxins alpha and beta (Supplementary Figure 2G). Further, and in conjunction with higher levels of Catch22 in NKp46^{-} ckit^{hi} than NKp46^{+} ILCs, ckit^{hi} ILCs constitutively expressed higher levels of the lineage determinant RORγt (Supplementary Figure 2H) and the activation marker CD69 (Figure 1F). Finally, without exogenous stimulation Catch22^{hi} cells and NKp46^{-} ckit^{hi} ILCs produced more IL-22 protein

(Figure 1G) and *Il22* message (Supplementary Figure 2G) than their counterparts. Thus, by comparing Catch22 and IL-22 signal intensity between immunofluorescent microscopy and flow cytometry we infer that Catch22^{hi} cells were LTi cells residing in SILT, whereas Catch22^{lo} cells were T cells and NKp46^{+} ILC3s dispersed throughout the villus lamina propria. Further, we find that SILT in the resting small intestine identified focal areas of immune activity characterized by highly-activated CD69^{+}, IL-22-expressing LTi cells, myeloid cell clustering, and activated stromal cells (VCAM1^{+}), even in the absence of infectious challenge.

LTi cell activation is concurrent with weaning

That SILT exhibited uniquely high levels of Catch22 expression was striking, as the common understanding of homeostatic IL-22 activity is in regulating epithelial antimicrobial tone, for example through induction of Reg3γ throughout the small intestine (2). In addition, current models of SILT activity suggest that CPs are quiescent until they are induced by enteric microbes to develop into ILFs (1). Our data, however, indicated a refinement of this model such that CPs are in a constitutively active state prior to the induction of ILFs. To determine when this activity was initiated, we monitored spontaneous Catch22 fluorescence in the developing intestine. Catch22^{+} cells were present in prenatal mice at Peyer's patch anlagen, though MFI was low (data not shown). Low MFI persisted until around weaning (post-natal day 21), when Catch22 MFI dramatically increased in T cells, NKp46^{+} ILC3s, and LTi cells to levels seen in adult animals (Figures 2A and Supplementary Figure 3A–C). LTi cells expressed higher levels of Catch22 and CD69 (Figure 2B) following weaning, indicating that IL-22 activation signals were concurrent with weaning.

Concordantly with Catch22 expression and LTi cell activation, transcript analysis from unfractionated distal ileum demonstrated increases in *Il17a*, *Il22ra2* (IL-22 binding protein, IL-22BP), and the STAT3 target *Wfdc18* (26) following weaning (Figure 2C). *Il17a* is particularly interesting, as previous work has shown that among ILC3s *Il17a* is restricted to NKp46^{-} cells (3, 27). We found that, like *Il22*, *Il17a* is induced upon weaning, is enriched in punch-dissected SILT, and is strongly reduced in the tissue when Catch22-expressing cells are deleted after crossing to a *Rosa26-DTa* allele (Figure 2C–F), which lack SILT (Supplementary Figure 3D–G). Likewise, whereas IL-22 receptor (*Il22ra1*) did not show preferential distribution (data not shown), transcript for IL-22 binding protein (*Il22ra2*), a negative regulator of IL-22 signaling (5), was also very highly enriched at SILT and dependent on Catch22-expressing cells (Figure 2D, 2F). Thus, weaning is accompanied by a marked increase in immune activity highlighted by LTi cell activation and type 3 cytokine activity at SILT.

SILT-localized *Il22* activity is dependent on MyD88 signaling in myeloid cells and epithelium

It is thought that pathogenic microbes induce quiescent CPs to recruit B cells and that the resulting ILFs generate protective IgA in an LTi cell-dependent manner (28). Given the profound changes in the microbiota following weaning, we speculated that microbial sensing was also responsible for the vigorous activation of the *Il22* locus at SILT in the healthy intestine. To determine whether a replete microbial flora was responsible not only for ILF

development but also for pre-ILF SILT activation, we treated mice with broad-spectrum antibiotics from fetal through post-wean life. Suppression of the microbiota by antibiotics profoundly reduced the number of Catch22^{hi} LTi cells, as well as the MFI of those that remained (Figure 3A, 3B). This phenotype was also observed when antibiotics were given to adults (data not shown), demonstrating a constitutively active pathway that is not restricted to a developmental window. Consistent with the normal development of CPs in germ-free mice shown by others (17), the total numbers of ILC3 subsets were normal in antibiotics-treated mice and Catch22^{dim} SILT were present in thin sections of small intestine (data not shown).

Microbial sensing in the intestine occurs in multiple cellular compartments, many of which utilize the signaling adaptor MyD88 downstream of toll-like receptors (TLR). We bred MyD88-flox mice to two Cre-expressing strains and monitored cellular activation using Catch22 fluorescence. Genetic deficiency of MyD88 in CD11c^{+} and Villin^{+} cells each resulted in a 50–70% reduction in Catch22 MFI in LTi cells (Figure 3C–F). Lack of MyD88 in CD11c^{+} cells led to impaired Catch22 activation in NKp46^{+} ILC3 and LTi cells, whereas lack of MyD88 in Villin^{+} cells impaired Catch22 expression only in LTi cell subset of ILC3. Catch22 was normal in IL-1 receptor knockout and IL-18 receptor knockout mice (Supplementary Figure 3H–I) and preliminary data suggest Asc knockout mice and mice deficient in IL-33 or IL-33 signaling have normal Catch22 or IL-22 levels at homeostasis (data not shown). These data suggest that TLR signaling was likely upstream of MyD88 at steady-state, though we have not formally excluded all other MyD88-dependent signaling pathways. Thus, like lamina propria-resident populations, steady-state LTi cells resident at SILT are dependent on the microbiota and MyD88 signaling for their activation.

Activated macrophages co-localize with LTi cells at SILT

To define the cellular components upstream of Catch22 and SILT activation, we analyzed mice that express YFP under control of the endogenous *Il12b* (IL-12/23 p40) locus, known as ‘Yet40’ (‘Y40’) (29). *Il12b* is activated downstream of TLR signaling and there are known sources of both IL-12 and IL-23 within the intestine. In the context of colonization with segmented filamentous bacteria (30) or during *Citrobacter rodentium* infection (7), IL-23^{+} cells are suggested to be distributed across affected epithelium. In the healthy, steady-state small intestine, however, we found Yet40^{+} cells preferentially, though not exclusively, residing in discrete clusters with Catch22^{+} cells (Figure 4A–D). In thin section the Yet40^{+} cell clusters were clearly SILT (Figure 4E), corroborating evidence that SILT represent sites of immune activation in the healthy intestine.

Yet40^{+} cells conformed to the phenotype of intestinal macrophages (31, 32) in that they expressed high levels of MHCII, CD11b, CD64, CD172a (SIRPα), F4/80, and MerTK, and expressed intermediate levels of CD11c and CD103 (Figure 5A and Supplementary Figure 4A), were positive for intracellular TLR3 and TLR9 (Supplementary Figure 4B), and expressed low levels of *Zbtb46* transcript (Figure 5B). Consistent with an intestinal macrophage phenotype, they also expressed higher levels of *Il10* and *Tnfa* than intestinal dendritic cells (CD11b$^{lo/-}$ CD11c^{hi} MHCII^{+}). Although a large number of MHCII^{+} cells in the small intestine are macrophages (CD11b^{+} CD11c^{int} CD64^{+}), only 3–5% were also

Yet40$^+$ (data not shown), and it was these cells which harbored most of the IL-23 potential as well as higher levels of IL-1β and IL-6. It was intriguing that Yet40$^+$ macrophages were also a major source of the IL-22 decoy receptor IL-22BP (*Il22ra2*) (Figure 5B **and** Supplementary Figure 4C) that we found to be highly enriched at SILT (Figure 2D), suggesting their potential to negatively regulate the IL-22 activity of SILT-resident LTi cells.

IL-12/23 p40 is a subunit of both IL-12 and IL-23. In order to determine whether Yet40 activation was indicative of IL-12 and/or IL-23 production, we compared sorted Yet40$^+$ and Yet40$^-$ macrophages. Transcript analysis of sorted MHCII$^+$ APCs indicated *Il23a* transcript segregated to the Yet40$^+$ cells with little, if any, *Il12a* expression detected in any population (Figure 5B). Previous work indicated that CpG oligodeoxynucleotides (CpG) elicited IL-22 from ILC3s co-cultured with intestinal macrophages via IL-23 (7). In accordance with this observation, we confirmed that CpG induced IL-23 production from macrophage cultures (Figure 6); however, only the small pool of Yet40$^+$ macrophages released IL-23 in response to CpG. By contrast, the TLR3 agonist poly(I:C) was capable of inducing IL-23 production from macrophages regardless of pre-existing *Il12b* activity. Yet40$^+$ macrophages also showed elevated production of IL-6 and TNF. Appreciable quantities of IL-12 were not detected under any of these conditions, suggesting that Yet40 expression in macrophages *in vivo* correlates with anatomic sites of IL-23 activity. These data demonstrate the existence of a coordinated interaction at SILT between Catch22^{hi} LTi cells and activated macrophages capable of regulating them via IL-23.

CpG induces adult-like IL-22 activity prior to weaning

Similarities in micro-anatomic location and activation status between Catch22$^+$ and Yet40$^+$ cells suggested these two cell types were coordinately regulated at SILT in steady-state mouse intestine and led us to speculate that Yet40$^+$ macrophages would exhibit similar pre-to-post-weaning regulation as Catch22$^+$ LTi cells. This hypothesis was not supported, however, as Yet40 reporter MFI was similar in pre- and post-weaned mice (Figure 7A). Despite this, Yet40$^+$ APCs exhibited a dramatic increase in number in the peri-weaning period (Figure 7B), coincident with the period of constitutive monocyte recruitment into the intestinal macrophage pool (33).

Constant YFP signal between pre- to post-wean Yet40$^+$ macrophages and the lack of detectable cytokines from *in vitro* cultures without addition of TLR stimulus suggested that the YFP signal seen in steady-state macrophages did not indicate continual cytokine secretion. Rather, it likely represented either a primed state or episodic activation that was undetectable at the population level. In spite of this, Yet40$^+$ macrophages were found in pre-activated SILT with Catch22^{dim} cells prior to weaning (Figure 7C–D) and we speculated that these cells would be capable of inducing Catch22 upon receipt of appropriate activating signals, as might occur due to changes in the microbiota following weaning. To test this, we treated neonatal mice with two consecutive doses of PBS, IL-23, CpG, or poly(I:C) and assessed Catch22 expression. Both IL-23 and CpG induced Catch22 in nearly all LTi cells (Figure 7E), and to a lesser extent T cells and NKp46$^+$ ILC3 (Supplementary Figure 4D), while poly(I:C) affected only a fraction of LTi cells. More striking, however, was the ability of CpG to induce adult-like levels of Catch22, in contrast to both IL-23 and poly(I:C)

(Figure 7F). These data suggest that, upon weaning, co-localized Catch22$^+$ LTi cells and Yet40$^+$ macrophages can respond to specific microbial signals to initiate IL-22 signaling at specialized foci of the intestinal tissue.

DISCUSSION

Using sensitive genetic cytokine reporter mice we identify previously unrecognized homeostatic activity in the intestine and provide anatomic resolution as to where these activities are focused. These observations were highlighted by the co-localization of highly active, IL-22-expressing LTi cells and primed macrophages at anatomically segregated SILT structures. This macrophage subset produced more cytokine in response to TLR stimulation *in vitro* and MyD88 deficiency in these cells abrogated LTi cell activation *in vivo*. Although both LTi cells and macrophages were present at SILT early in life this circuit remained quiescent until weaning, thereby identifying pre-ILF SILT structures as anatomically-restricted immune hubs that couple sensing of microbial signals with tightly regulated immunologic maturation during this critical developmental milestone.

Recently, two other *Il22* reporter mice were generated. Analysis of these reagents either focused on T cells (24) or utilized the *Il22* locus to fate-map cells (23), which prevented observations of transcriptional intensity and temporal control. In contrast, we focused on real-time *Il22* activity, with particular attention to reporter intensity and spatial distribution of reporter-positive cells. This allowed us to make two novel observations regarding IL-22 production by intestinal ILC3s. First, LTi cells in the healthy intestine were more active than their NKp46$^+$ counterparts. The potency of LTi cells for IL-22 production has been noted in the literature (34–36), but thus far an appreciation of this distinction and their particular anatomic distribution in SILT is not integrated into models of ILC3 activity and intestinal homeostasis. Though NKp46$^+$ ILC3 have been found at small SILT(8), our data is in accordance with a recent report demonstrating that NKp46$^+$ and lamina propria ILC3 are controlled by the chemokine receptor CXCR6, whereas LTi cells and SILT-resident ILC3 are not(13), reflecting a functional and anatomic axis highlighted by our work. The Catch22 allele allowed us to functionally identify NKp46$^-$ ILC3s irrespective of CD4 expression and easily localize their distribution within the small intestine, and clearly indicated the dominant capacity of LTi cells for IL-22 production and heightened activity in healthy intestine. Indeed, although the importance of NKp46$^+$ ILC3s in many processes is well supported, recent studies suggest an unappreciated contribution from LTi cells in commonly used models of intestinal pathology (4, 34). These data together with our observations prompt a reevaluation of disease susceptibility in germ-line knockout mice (*Il22*, *Rorc*, *Ahr*, lymphotoxin), which may have an altered baseline intestinal immune tone owing to disrupted LTi cells and/or IL-22 activity, as was demonstrated (9).

Second, use of the Catch22 allele revealed the kinetics of SILT activation. SILT-resident LTi cell activation coincided with weaning and it was dependent on a replete intestinal flora, MyD88 signaling in CD11c$^+$ and Villin$^+$ cells, and did not require IL-1 receptor or IL-18 receptor. Preliminary data also suggests other IL-1 family members are not required for steady-state LTi cell activation, suggesting that cells at SILT actively survey the microbiota and elicit *Il22* activity regardless of SILT size or the presence or absence of B cells.

Therefore, our work adds to a number of previous studies (37–42) highlighting the importance of a replete intestinal flora for steady-state IL-22 levels. These results are, however, contradicted by a previous report (43) showing diminishing activity from LTi cells taken from 8 week-old compared to 2 week-old mice, and suppression of IL-22 by the microbiota. We cannot resolve this contradiction but it is possible that stimulation of the cells in that study, as opposed to *ex vivo* and *in situ* analysis in our work, or institutional colony differences, could be responsible.

The observed activation event at SILT upon weaning is a significant refinement to the current model of secondary lymphoid tissue development in gut lamina propria, which posits that microbial sensing and activation directly leads to the generation of a B cell follicle (18, 19). We identified a microbiota-regulated activation event at SILT exclusive of that which induces a B cell follicle, as evidenced by LTi cell activation irrespective of SILT size or follicle development. Nevertheless, microbial sensing is necessary for the induction of a B cell follicle at SILT and IL-22 is important to this process (44), at least in the large intestine. Therefore, we hypothesize that two microbiota-dependent activation events operate on SILT: 1) a signal received by small, quiescent SILT at weaning leading to activation of LTi and possibly other cells, and 2) a signal received by small, activated SILT leading to B cell recruitment and elaboration of a productive follicle. Future studies should be directed toward identifying what distinguishes these two microbiota-dependent events, as the latter may involve inflammatory signals generated by tissue damage or cytoplasmic microbial sensing as would occur following pathogenic insults.

Use of Yet40 reporter mice, which express YFP from the *Il12b* locus, provided a way of observing a functional-anatomic link within the large macrophage population of the small intestine. Yet40 mice revealed that a small fraction of intestinal APCs were activated at steady-state and anatomically segregated with IL-22-expressing SILT-resident LTi cells. We did not observe SILT of any size that did not also harbor Yet40^{+} cells. Thus, at least three activated populations reside at SILT at steady-state: VCAM1^{+} stromal cells (25), Catch22^{+} LTi cells, and Yet40^{+} APCs. Yet40^{+} cells also accumulated through the peri-weaning period, suggesting that the induction of Catch22 at SILT coincided with Yet40 residency at these structures. We did not find an increase in Yet40 MFI to mirror that of Catch22, but it is formally possible that during weaning the Yet40^{+} pool reaches a critical mass at SILT for induction of Catch22^{hi} LTi cells. Other formal possibilities coincident with weaning are the induction of an accessory factor (other than *Il12b*) in Yet40^{+} cells or other SILT-resident cells, or release of an inhibitory “brake” on LTi cell activation, though we did not address these possibilities.

Yet40^{+} small intestine APCs were identified as macrophages based upon a variety of markers and the lack of *Zbtb46* transcript associated with the DC lineage (31, 32). Small intestine Yet40^{+} macrophages were more responsive to TLR stimulation than their Yet40^{-} counterparts and were capable of producing factors, e.g., IL-23, which potently activated LTi cells. The identification of this small fraction of Yet40^{+} macrophages as part of a steady-state network of IL-22 production expands upon previous work (11) and is a significant advancement over existing genetic tools (*e.g.*, CD11c, CX3CR1) which label a majority of

APCs in the intestine (22). Our findings enable a significantly more refined analysis of IL-22-dependent homeostasis and immune activation.

In concordance with previous studies (7), *in vitro* stimulation with TLR9 ligand CpG had the most profound effect on Yet40$^+$ macrophages. The ability of CpG to elicit substantial levels of IL-12/23 p40 and IL-23 exclusively from Yet40$^+$ macrophages *in vitro* and induce adult-like levels of Catch22 from neonatal mice *in vivo* suggests that TLR9 has an important role in establishing and maintaining steady-state IL-22 production. In fact, prior reports identified a role for CpG/TLR9 in wound healing and intestinal tolerance (45–47), implicating Yet40$^+$ macrophages in these protective responses. While these studies did not assess IL-22 levels or SILT activation, our data suggest one consequence of CpG administration is the activation of SILT-resident macrophages. In fact, islet allograft survival is enhanced by CpG administration resulting in enhanced IL-23 and IL-22 production (48). Therefore, Yet40$^+$ macrophages residing in SILT may be able to acquire and detect microbial products for the production of tissue-protective factors.

Curiously, these same macrophages also appear to be a major source of steady-state IL-22BP. Our data demonstrate that in the small intestine *Il22ra2* transcript anatomically correlated with SILT, genetically depended on the presence of SILT, and was expressed much more highly in Yet40$^+$ macrophages than in other macrophages, dendritic cells, or T cells. A recent report confirms some of these findings(49). This additional layer of IL-22 regulation appeared in concert with induction of IL-22 activity, as it appeared after weaning. IL-22BP negatively regulates IL-22 activity (50, 51) and was shown to limit chemically-induced colon carcinomas (52). Additionally, it was previously shown that IL-22BP expression is induced by retinoic acid (53) and suppressed by IL-18 (52), both of which are known epithelial products also linked to IL-22 activity (54–56). These observations suggest a model whereby SILT are signal integration platforms organized around microbe-sensing Yet40$^+$ macrophages that represent both sources of IL-23 and IL-22BP, and potential regulatory targets of retinoic acid and IL-18.

Though study of intestinal ILC3s and macrophage populations continues to be hampered by a lack of specific tools, the resolution provided by these functionally-encoded genetic models allowed us to observe developmental and homeostatic processes not previously appreciated. Whether this system in mouse reflects human biology remains unclear. It is generally considered that there are no CPs in human intestine (16), though recent evidence questions this conclusion (57, 58) and it is possible that the widespread CPs present in mouse intestine reflects a human developmental stage captured in specific pathogen-free mouse colonies. Irrespective of a direct CP correlate, human as well as mouse intestine commonly exhibit hyper-cellular, engorged, villi containing abundant APCs and VCAM1$^+$ stromal cells, as well as IL-22-expressing cells ((59, 60) and data not shown). While the etiology and function of these structures are unknown, their common cellular constituents may indicate pathways shared with CP and ILF development. Future work focusing on the interactions occurring between activated macrophages and IL-22-producing LTi cells during SILT progression and at inflammatory foci will be important in unraveling the pre-emptive formation of such structures and the capacity to sustain intestinal homeostasis. The tools we describe will be important in examining this process.

Supplementary Material

Refer to Web version on PubMed Central for supplementary material.

Acknowledgments

A.K.S. conceived the study, designed and performed experiments, and analyzed the data. H.-E.L. cloned the Catch22 reporter cassette and performed the Catch22 embryonic stem cell work. R.M.L. directed the study and wrote the paper with A.K.S. We thank Z. Wang, M. Ji, M. Consengco, and N. Flores for technical expertise; Z. Wang, J. Schanin, and members of the Locksley laboratory for helpful discussions. R. Taniguchi, A. Molofsky, S. van Dyken, and J. Nussbaum provided helpful comments on the manuscript.

References

1. Dudakov JA, Hanash AM, van den Brink MRMM. Interleukin-22: Immunobiology and Pathology. Annu Rev Immunol. 2015; 33:747–85. [PubMed: 25706098]
2. Zheng Y, Valdez PA, Danilenko DM, Hu Y, Sa SM, Gong Q, Abbas AR, Modrusan Z, Ghilardi N, de Sauvage FJ, Ouyang W. Interleukin-22 mediates early host defense against attaching and effacing bacterial pathogens. Nat Med. 2008; 14:282–9. [PubMed: 18264109]
3. Rankin LC, Girard-Madoux MJH, Seillet C, Mielke LA, Kerdiles Y, Fenis A, Wieduwild E, Putoczki T, Mondot S, Lantz O, Demon D, Papenfuss AT, Smyth GK, Lamkanfi M, Carotta S, Renauld JC, Shi W, Carpentier S, Soos T, Arendt C, Ugolini S, Huntington ND, Belz GT, Vivier E. Complementarity and redundancy of IL-22-producing innate lymphoid cells. Nat Immunol. 2016; 17:179–86. [PubMed: 26595889]
4. Song C, Lee JS, Gilfillan S, Robinette ML, Newberry RD, Stappenbeck TS, Mack M, Cella M, Colonna M. Unique and redundant functions of NKp46+ ILC3s in models of intestinal inflammation. J Exp Med. 2015; 212:1869–82. [PubMed: 26458769]
5. Sugimoto K, Ogawa A, Mizoguchi E, Shimomura Y, Andoh A, Bhan AK, Blumberg RS, Xavier RJ, Mizoguchi A. IL-22 ameliorates intestinal inflammation in a mouse model of ulcerative colitis. J Clin Invest. 2008; 118:534–44. [PubMed: 18172556]
6. Zenewicz LA, Yancopoulos GD, Valenzuela DM, Murphy AJ, Stevens S, Flavell Ra. Innate and Adaptive Interleukin-22 Protects Mice from Inflammatory Bowel Disease. Immunity. 2008; 29:947–957. [PubMed: 19100701]
7. Longman RS, Diehl GE, Victorio Da, Huh JR, Galan C, Miraldi ER, Swaminath A, Bonneau R, Scherl EJ, Littman DR. CX3CR1+ mononuclear phagocytes support colitis-associated innate lymphoid cell production of IL-22. J Exp Med. 2014; 211:1571–83. [PubMed: 25024136]
8. Sanos SL V, Bui L, Mortha A, Oberle K, Heners C, Johner C, Diefenbach A. RORgammat and commensal microflora are required for the differentiation of mucosal interleukin 22-producing NKp46+ cells. Nat Immunol. 2009; 10:83–91. [PubMed: 19029903]
9. Zenewicz, La, Yin, X., Wang, G., Elinav, E., Hao, L., Zhao, L., Flavell, Ra. IL-22 Deficiency Alters Colonic Microbiota To Be Transmissible and Colitogenic. J Immunol. 2013; 190:5306–12. [PubMed: 23585682]
10. Autenrieth SE, Warnke P, Wabnitz GH, Lucero Estrada C, Pasquevich KA, Drechsler D, Günter M, Hochweller K, Novakovic A, Beer-Hammer S, Samstag Y, Hämmerling GJ, Garbi N, Autenrieth IB. Depletion of dendritic cells enhances innate anti-bacterial host defense through modulation of phagocyte homeostasis. PLoS Pathog. 2012; 8:e1002552. [PubMed: 22383883]
11. Kinnebrew MA, Buffie CG, Diehl GE, Zenewicz LA, Leiner I, Hohl TM, Flavell RA, Littman DR, Pamer EG. Interleukin 23 production by intestinal CD103(+)CD11b(+) dendritic cells in response to bacterial flagellin enhances mucosal innate immune defense. Immunity. 2012; 36:276–287. [PubMed: 22306017]
12. Medina-Contreras O, Geem D, Laur O, Williams IR, Lira SA, Nusrat A, Parkos CA, Denning TL. CX3CR1 regulates intestinal macrophage homeostasis, bacterial translocation, and colitogenic Th17 responses in mice. J Clin Invest. 2011; 121:4787–95. [PubMed: 22045567]

13. Satoh-Takayama N, Serafini N, Verrier T, Rekiki A, Renauld JC, Frankel G, Di Santo JP. The Chemokine Receptor CXCR6 Controls the Functional Topography of Interleukin-22 Producing Intestinal Innate Lymphoid Cells. Immunity. 2014; 41:776–788. [PubMed: 25456160]
14. Eberl G. Inducible lymphoid tissues in the adult gut: recapitulation of a fetal developmental pathway? Nat Rev Immunol. 2005; 5:413–20. [PubMed: 15841100]
15. Pabst O, Herbrand H, Friedrichsen M, Velaga S, Dorsch M, Berhardt G, Worbs T, Macpherson AJ, Förster R. Adaptation of solitary intestinal lymphoid tissue in response to microbiota and chemokine receptor CCR7 signaling. J Immunol. 2006; 177:6824–32. [PubMed: 17082596]
16. Pabst O, Herbrand H, Worbs T, Friedrichsen M, Yan S, Hoffmann MW, Körner H, Bernhardt G, Pabst R, Förster R. Cryptopatches and isolated lymphoid follicles: dynamic lymphoid tissues dispensable for the generation of intraepithelial lymphocytes. Eur J Immunol. 2005; 35:98–107. [PubMed: 15580658]
17. Kanamori Y. Identification of novel lymphoid tissues in murine intestinal mucosa where clusters of c-kit+ IL-7R+ Thy1+ lympho-hemopoietic progenitors develop. J Exp Med. 1996; 184:1449–1459. [PubMed: 8879216]
18. Lorenz RG, Chaplin DD, McDonald KG, McDonough JS, Newberry RD. Isolated lymphoid follicle formation is inducible and dependent upon lymphotoxin-sufficient B lymphocytes, lymphotoxin beta receptor, and TNF receptor I function. J Immunol. 2003; 170:5475–5482. [PubMed: 12759424]
19. Bouskra D, Brézillon C, Bérard M, Werts C, Varona R, Boneca IG, Eberl G. Lymphoid tissue genesis induced by commensals through NOD1 regulates intestinal homeostasis. Nature. 2008; 456:507–510. [PubMed: 18987631]
20. Rutz S, Wang X, Ouyang W. The IL-20 subfamily of cytokines — from host defence to tissue homeostasis. Nat Rev Immunol. 2014; 14:783–795. [PubMed: 25421700]
21. Shih VFS, Cox J, Kljavin NM, Dengler HS, Reichelt M, Kumar P, Rangell L, Kolls JK, Diehl L, Ouyang W, Ghilardi N. Homeostatic IL-23 receptor signaling limits Th17 response through IL-22-mediated containment of commensal microbiota. Proc Natl Acad Sci U S A. 2014; 111:13942–7. [PubMed: 25201978]
22. Bain CC, Mowat AM. The monocyte-macrophage axis in the intestine. Cell Immunol. 2014; 291:41–8. [PubMed: 24726741]
23. Ahlfors H, Morrison PJ, Duarte JH, Li Y, Biro J, Tolaini M, Di Meglio P, Potocnik AJ, Stockinger B. IL-22 Fate Reporter Reveals Origin and Control of IL-22 Production in Homeostasis and Infection. J Immunol. 2014; 193:4602–4613. [PubMed: 25261485]
24. Shen W, Hixon JA, McLean MH, Li WQ, Durum SK. IL-22-Expressing Murine Lymphocytes Display Plasticity and Pathogenicity in Reporter Mice. Front Immunol. 2015; 6:662. [PubMed: 26834739]
25. Taylor RT, Lugering A, Newell KA, Williams IR. Intestinal Cryptopatch Formation in Mice Requires Lymphotoxin and the Lymphotoxin Receptor. J Immunol. 2004; 173:7183–7189. [PubMed: 15585839]
26. Pickert G, Neufert C, Leppkes M, Zheng Y, Wittkopf N, Warntjen M, Lehr HA, Hirth S, Weigmann B, Wirtz S, Ouyang W, Neurath MF, Becker C. STAT3 links IL-22 signaling in intestinal epithelial cells to mucosal wound healing. J Exp Med. 2009; 206:1465–72. [PubMed: 19564350]
27. Robinette ML, Fuchs A, Cortez VS, Lee JS, Wang Y, Durum SK, Gilfillan S, Colonna M. Immunological Genome Consortium, and G. Consortium. Transcriptional programs define molecular characteristics of innate lymphoid cell classes and subsets. Nat Immunol. 2015; 16:306–17. [PubMed: 25621825]
28. Knoop KA, Newberry RD. Isolated Lymphoid Follicles are Dynamic Reservoirs for the Induction of Intestinal IgA. Front Immunol. 2012; 3:84. [PubMed: 22566964]
29. Reinhardt RL, Hong S, Kang S-J, Wang Z-eZ, Locksley RM. Visualization of IL-12/23p40 in vivo reveals immunostimulatory dendritic cell migrants that promote Th1 differentiation. J Immunol. 2006; 177:1618–1627. [PubMed: 16849470]
30. Ivanov II, Atarashi K, Manel N, Brodie EL, Shima T, Karaoz U, Wei D, Goldfarb KC, Santee CA, Lynch SV, Tanoue T, Imaoka A, Itoh K, Takeda K, Umesaki Y, Honda K, Littman DR. Induction

of intestinal Th17 cells by segmented filamentous bacteria. Cell. 2009; 139:485–98. [PubMed: 19836068]

31. Persson EK, Scott CL, Mowat AM, Agace WW. Dendritic cell subsets in the intestinal lamina propria: ontogeny and function. Eur J Immunol. 2013; 43:3098–107. [PubMed: 23966272]
32. Tamoutounour S, Henri S, Lelouard H, de Bovis B, de Haar C, van der Woude CJ, Woltman AM, Reyal Y, Bonnet D, Sichien D, Bain CC, Mowat AM, Reis e Sousa C, Poulin LF, Malissen B, Guilliams M. CD64 distinguishes macrophages from dendritic cells in the gut and reveals the Th1-inducing role of mesenteric lymph node macrophages during colitis. Eur J Immunol. 2012; 42:3150–66. [PubMed: 22936024]
33. Bain CC, Bravo-Blas A, Scott CL, Gomez Perdiguero E, Geissmann F, Henri S, Malissen B, Osborne LC, Artis D, Mowat AM. Constant replenishment from circulating monocytes maintains the macrophage pool in the intestine of adult mice. Nat Immunol. 2014; 15:929–37. [PubMed: 25151491]
34. Sonnenberg GF, Monticelli La, Elloso MM, Fouser La, Artis D. CD4+ Lymphoid Tissue-Inducer Cells Promote Innate Immunity in the Gut. Immunity. 2011; 34:122–134. [PubMed: 21194981]
35. Tumanov AV, Koroleva EP, Guo X, Wang Y, Kruglov A, Nedospasov S, Fu YX. Lymphotoxin controls the IL-22 protection pathway in gut innate lymphoid cells during mucosal pathogen challenge. Cell Host Microbe. 2011; 10:44–53. [PubMed: 21767811]
36. Marchesi F, Martin aP, Thirunarayanan N, Devany E, Mayer L, Grisotto MG, Furtado GC, Lira SA. CXCL13 expression in the gut promotes accumulation of IL-22-producing lymphoid tissue-inducer cells, and formation of isolated lymphoid follicles. Mucosal Immunol. 2009; 2:486–494. [PubMed: 19741597]
37. Hernández-Chirlaque C, Aranda CJ, Ocón B, Capitán-Cañadas F, Ortega-González M, Carrero JJ, Suárez MD, Zarzuelo A, Sánchez de Medina F, Martínez-Augustin O. Germ-free and Antibiotic-treated Mice are Highly Susceptible to Epithelial Injury in DSS Colitis. J Crohn's Colitis. 2016; 10:1324–1335. [PubMed: 27117829]
38. Fung TC, Bessman NJ, Hepworth MR, Kumar N, Shibata N, Kobuley D, Wang K, Ziegler CGK, Goc J, Shima T, Umesaki Y, Sartor RB, Sullivan KV, Lawley TD, Kunisawa J, Kiyono H, Sonnenberg GF. Lymphoid-Tissue-Resident Commensal Bacteria Promote Members of the IL-10 Cytokine Family to Establish Mutualism. Immunity. 2016; 44:634–646. [PubMed: 26982365]
39. Grasberger H, Gao J, Nagao-Kitamoto H, Kitamoto S, Zhang M, Kamada N, Eaton KA, El-Zaatari M, Shreiner AB, Merchant JL, Owyang C, Kao JY. Increased Expression of DUOX2 Is an Epithelial Response to Mucosal Dysbiosis Required for Immune Homeostasis in Mouse Intestine. Gastroenterology. 2015; 149:1849–59. [PubMed: 26261005]
40. Zelante T, Iannitti RG, Cunha C, De Luca A, Giovannini G, Pieraccini G, Zecchi R, D'Angelo C, Massi-Benedetti C, Fallarino F, Carvalho A, Puccetti P, Romani L. Tryptophan catabolites from microbiota engage aryl hydrocarbon receptor and balance mucosal reactivity via interleukin-22. Immunity. 2013; 39:372–85. [PubMed: 23973224]
41. Verrier T, Satoh-Takayama N, Serafini N, Marie S, Di Santo JP, Vosshenrich CAJ. Phenotypic and Functional Plasticity of Murine Intestinal NKp46+ Group 3 Innate Lymphoid Cells. J Immunol. 2016; 196:4731–4738. [PubMed: 27183613]
42. Satoh-Takayama N, Vosshenrich CaJ, Lesjean-Pottier S, Sawa S, Lochner M, Rattis F, Mention JJ, Thiam K, Cerf-Bensussan N, Mandelboim O, Eberl G, Di Santo JP. Microbial Flora Drives Interleukin 22 Production in Intestinal NKp46+ Cells that Provide Innate Mucosal Immune Defense. Immunity. 2008; 29:958–970. [PubMed: 19084435]
43. Sawa S, Lochner M, Satoh-Takayama N, Dulauroy S, Bérard M, Kleinschek M, Cua D, Di Santo JP, Eberl G. RORγt+ innate lymphoid cells regulate intestinal homeostasis by integrating negative signals from the symbiotic microbiota. Nat Immunol. 2011; 12:320–326. [PubMed: 21336274]
44. Ota N, Wong K, Valdez PA, Zheng Y, Crellin NK, Diehl L, Ouyang W. IL-22 bridges the lymphotoxin pathway with the maintenance of colonic lymphoid structures during infection with Citrobacter rodentium. Nat Immunol. 2011; 12:941–948. [PubMed: 21874025]
45. Zhang C, Ni J, Li BL, Gao F, Liu H, Liu W, Huang YJ, Cai JM. CpG-Oligodeoxynucleotide Treatment Protects against Ionizing Radiation-Induced Intestine Injury. PLoS One. 2013; 8:e66586. [PubMed: 23805241]

46. Lacroix-Lamandé S, Rochereau N, Mancassola R, Barrier M, Clauzon A, Laurent F. Neonate Intestinal Immune Response to CpG Oligodeoxynucleotide Stimulation. PLoS One. 2009; 4:e8291. [PubMed: 20011519]
47. Gribar SC, Sodhi CP, Richardson WM, Anand RJ, Gittes GK, Branca MF, Jakub A, Shi X-h, Shah S, Ozolek JA, Hackam DJ. Reciprocal Expression and Signaling of TLR4 and TLR9 in the Pathogenesis and Treatment of Necrotizing Enterocolitis. J Immunol. 2009; 182:636–646. [PubMed: 19109197]
48. Tripathi D, Venkatasubramanian S, Cheekatla SS, Paidipally P, Welch E, Tvinnereim AR, Vankayalapati R, Eizirik DL, Colli ML, Ortis F, Lehuen A, Diana J, Zaccone P, Cooke A, Jabs DA, Vial T, Descotes J, De Leeuw I, Merani S, Toso C, Emamaullee J, Shapiro AMJ, Hultkrantz S, Östman S, Telemo E, Donckier V, Knolle PA, Gerken G, Lau AH, Thomson AW, Krueger PD, Lassen MG, Qiao H, Hahn YS, Lassen MG, Lukens JR, Dolina JS, Brown MG, Hahn YS, Cooper MA, Colonna M, Yokoyama WM, Biassoni R, Yu G, Xu X, Vu MD, Kilpatrick ED, Li XC, Beilke JN, Kuhl NR, Van Kaer L, Gill RG, Cobleigh MA, Robek MD, Peng H, Hasnain SZ, Hall LJ, Colmenero P, Fallarino F, Puccetti P, Roda JM, Parihar R, Carson WE, Crispe IN, Bowen DG, Naziruddin B, Sakata N, Hamerman JA, Ogasawara K, Lanier LL, Vivier E, Nunès JA, Vély F, Roder JC, Kiessling R, Biberfeld P, Andersson B, Kitchens WH, Ishiyama K, Rawson J, Omori K, Mullen Y, Benichou G, Yamada Y, Aoyama A, Madsen JC, Zenewicz LA, Sonnenberg GF, Fouser LA, Artis D, Pan FHH, Hanash AM, Wolk K, Sabat R, Ouyang W, Wolk K, Colonna M, Fonseca SG, Gromada J, Urano F, Plesner A, Verchere CB, Wang X, Wolk K, Huszarik K, Brissova M, Gauthier BR, Lipson KL, Jinushi M, Hornung V, Kitagaki K, Businga TR, Kline JN, Fallarino F, Volpi C, Volpi C, Li DS, Yuan YH, Tu HJ, Liang QL, Dai LJ, Graham ML, Janecek JL, Kittredge JA, Hering BJ, Schuurman HJ, Barnett MJ, McGhee-Wilson D, Shapiro AMJ, Lakey JRT, Dhiman R, Müller M, Schreiber M, Kartenbeck J, Schreiber G, Berg RE, Crossley E, Murray S, Forman J, Kaufmann PM, Rabinovitch A, Venkatasubramanian S, Venkatasubramanian S. A TLR9 agonist promotes IL-22-dependent pancreatic islet allograft survival in type 1 diabetic mice. Nat Commun. 2016; 7:13896. [PubMed: 27982034]
49. Jinnohara T, Kanaya T, Hase K, Sakakibara S, Kato T, Tachibana N, Sasaki T, Hashimoto Y, Sato T, Watarai H, Kunisawa J, Shibata N, Williams IR, Kiyono H, Ohno H. IL-22BP dictates characteristics of Peyer's patch follicle-associated epithelium for antigen uptake. J Exp Med. 2017; 214:1607–1618. [PubMed: 28512157]
50. Wei CC, Ho TW, Liang WG, Chen GY, Chang MS. Cloning and characterization of mouse IL-22 binding protein. Genes Immun. 2003; 4:204–11. [PubMed: 12700595]
51. Pelczar P, Witkowski M, Perez LG, Kempski J, Hammel AG, Brockmann L, Kleinschmidt D, Wende S, Haueis C, Bedke T, Witkowski M, Krasemann S, Steurer S, Booth CJ, Busch P, König A, Rauch U, Benten D, Izbicki JR, Rösch T, Lohse AW, Strowig T, Gagliani N, Flavell RA, Huber S. A pathogenic role for T cell–derived IL-22BP in inflammatory bowel disease. Science. 2016; 354:358–362. [PubMed: 27846573]
52. Huber S, Gagliani N, Zenewicz LA, Huber FJ, Bosurgi L, Hu B, Hedl M, Zhang W, O'Connor W, Murphy AJ, Valenzuela DM, Yancopoulos GD, Booth CJ, Cho JH, Ouyang W, Abraham C, Flavell RA, Flavell RA. IL-22BP is regulated by the inflammasome and modulates tumorigenesis in the intestine. Nature. 2012; 491:259–63. [PubMed: 23075849]
53. Martin JCJ, Bériou G, Heslan M, Chauvin C, Utriainen L, Aumeunier a, Scott CL, Mowat a, Cerovic V, Houston Sa, Leboeuf M, Hubert FX, Hémont C, Merad M, Milling S, Josien R. Interleukin-22 binding protein (IL-22BP) is constitutively expressed by a subset of conventional dendritic cells and is strongly induced by retinoic acid. Mucosal Immunol. 2014; 7:101–13. [PubMed: 23653115]
54. Mielke LA, Jones Sa, Raverdeau M, Higgs R, Stefanska A, Groom JR, Misiak A, Dungan LS, Sutton CE, Streubel G, Bracken AP, Mills KHG. Retinoic acid expression associates with enhanced IL-22 production by γδ T cells and innate lymphoid cells and attenuation of intestinal inflammation. J Exp Med. 2013; 210:1117–24. [PubMed: 23690441]
55. Goverse G, Labao-Almeida C, Ferreira M, Molenaar R, Wahlen S, Konijn T, Koning J, Veiga-Fernandes H, Mebius RE. Vitamin A Controls the Presence of RORγ+ Innate Lymphoid Cells and Lymphoid Tissue in the Small Intestine. J Immunol. 2016; 196:5148–55. [PubMed: 27183576]
56. Muñoz M, Eidenschenk C, Ota N, Wong K, Lohmann U, Kühl AA, Wang X, Manzanillo P, Li Y, Rutz S, Zheng Y, Diehl L, Kayagaki N, van Lookeren-Campagne M, Liesenfeld O, Heimesaat M,

Ouyang W. Interleukin-22 Induces Interleukin-18 Expression from Epithelial Cells during Intestinal Infection. Immunity. 2015; 42:321–331. [PubMed: 25680273]

57. Nochi T, Denton PW, Wahl A, Garcia JV. Cryptopatches Are Essential for the Development of Human GALT. Cell Rep. 2013; 3:1874–1884. [PubMed: 23791525]
58. Lügering A, Ross M, Sieker M, Heidemann J, Williams IR, Domschke W, Kucharzik T. CCR6 identifies lymphoid tissue inducer cells within cryptopatches. Clin Exp Immunol. 2010; 160:440–449. [PubMed: 20148914]
59. McNamee EN, Masterson JC, Jedlicka P, Collins CB, Williams IR, Rivera-Nieves J. Ectopic lymphoid tissue alters the chemokine gradient, increases lymphocyte retention and exacerbates murine ileitis. Gut. 2013; 62:53–62. [PubMed: 22267601]
60. Moghaddami M, Cummins A, Mayrhofer G. Lymphocyte-filled villi: Comparison with other lymphoid aggregations in the mucosa of the human small intestine. Gastroenterology. 1998; 115:1414–1425. [PubMed: 9834269]

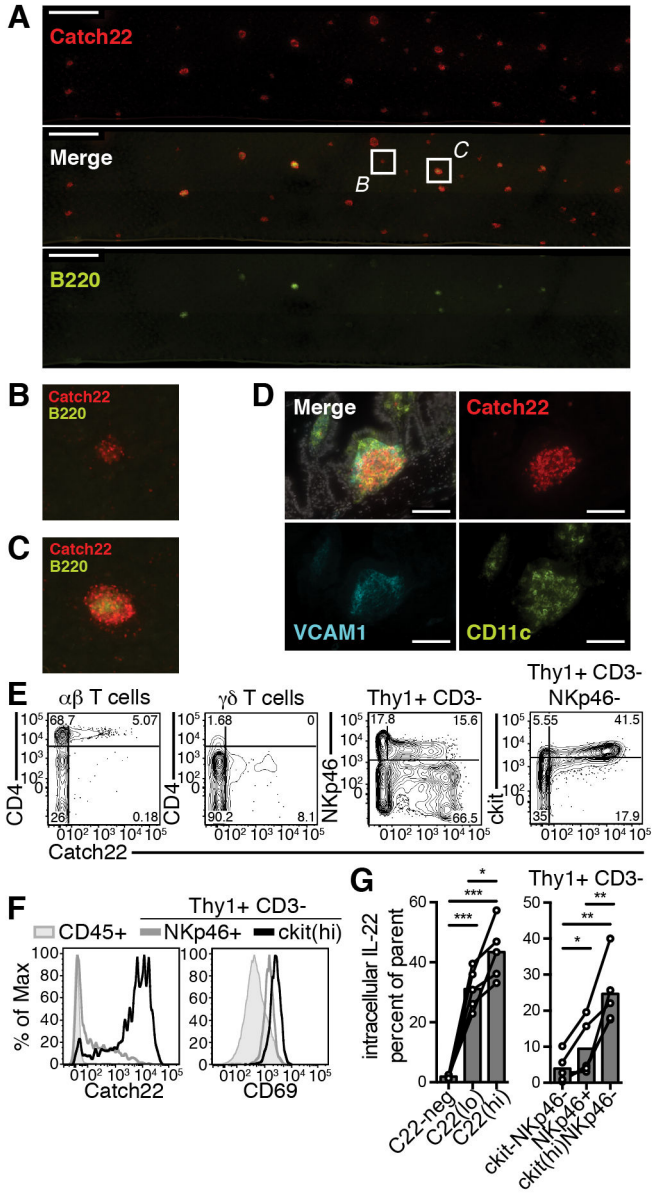

Figure 1.

Small intestine LTi cells are constitutively activated at SILT. (**A**) *Il22*$^{C22/+}$ murine small intestine was fixed and stained by whole mount for Catch22 (red) and B220 (green) (representative of n=2). Scale bar represents 1 mm. (**B,C**) Detail of the indicated regions from ***A*** to demonstrate small (**B**) and large (**C**) SILT structures. (**D**) Small intestine from *Il22*$^{C22/+}$ mice was fixed, sectioned, and stained for Catch22 (red), CD11c (green), VCAM1 (light blue), and DAPI (gray) (representative of n=5). Scale bar represents 100 μm. (**E**) Lymphocytes were isolated from the proximal third of small intestine lamina propria and analyzed for Catch22 fluorescence among CD45^{+} cells (representative of n=5). (**F**) ILC (Thy1^{+} CD3^{-}) subsets were analyzed for Catch22 and CD69 (representative of n=4–7). (**G**) Small intestine lamina propria cells were isolated in the presence of Brefeldin A and stained

for intracellular IL-22 without exogenous stimulation. Data connected by line are from the same mouse (n=5).

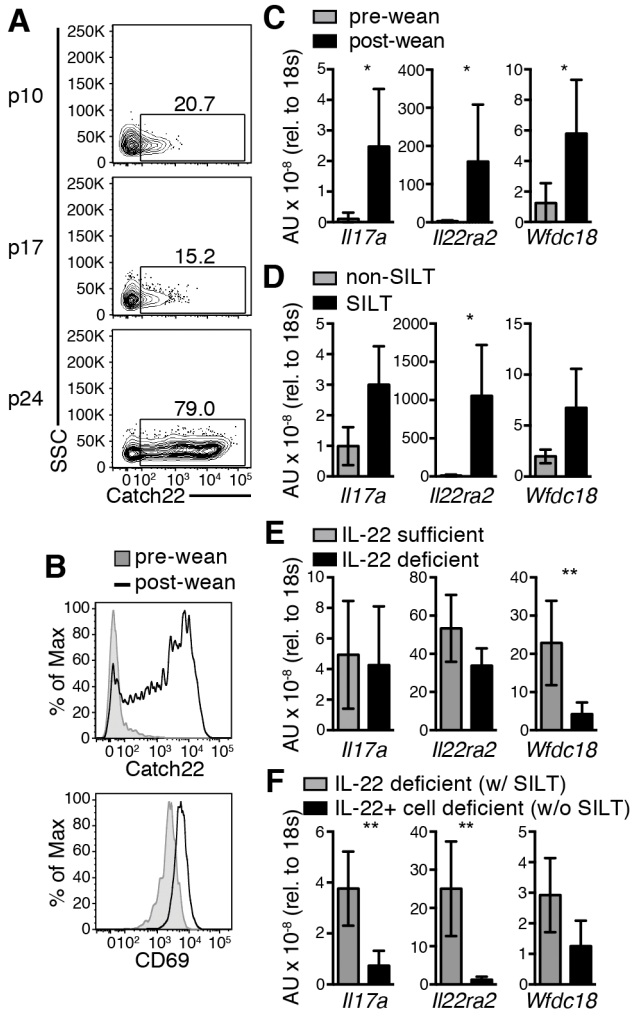

Figure 2.

LTi cell activation is induced upon weaning. (**A**) *Il22*$^{C22/+}$ small intestine lamina propria from 10–24 day-old mice was analyzed for Catch22 fluorescence in LTi cells. Peyer's patches were removed from p17 and p24, but not p10, mice. (representative of n=6–9 per time point). (**B**) Catch22 and CD69 expression levels on LTi cells were compared between pre- and post-wean mice (representative of n=6 each). (**C–F**) RNA/cDNA isolated from unfractionated distal ileum was processed for transcript analysis; from (**C**) pre- and post-wean mice (*Il22*$^{C22/+}$; n=3 each), (**D**) punch-dissected non-SILT and SILT from *Il22*$^{C22/+}$ mice (n=4–5 each), (**E**) IL-22 sufficient (*Il22*$^{C22/+}$) and deficient mice (*Il22*$^{C22/C22}$; n=5–6 each), and (**F**) IL-22 deficient mice with SILT (*Il22*$^{C22/C22}$) and mice which delete IL-22-expressing cells and don't have SILT (*Il22*$^{C22/C22}$*;Rosa*$^{DTa/+}$; n=4 each). The tissue did not include Peyer's patches. t test significance: * < 0.05, ** < 0.01.

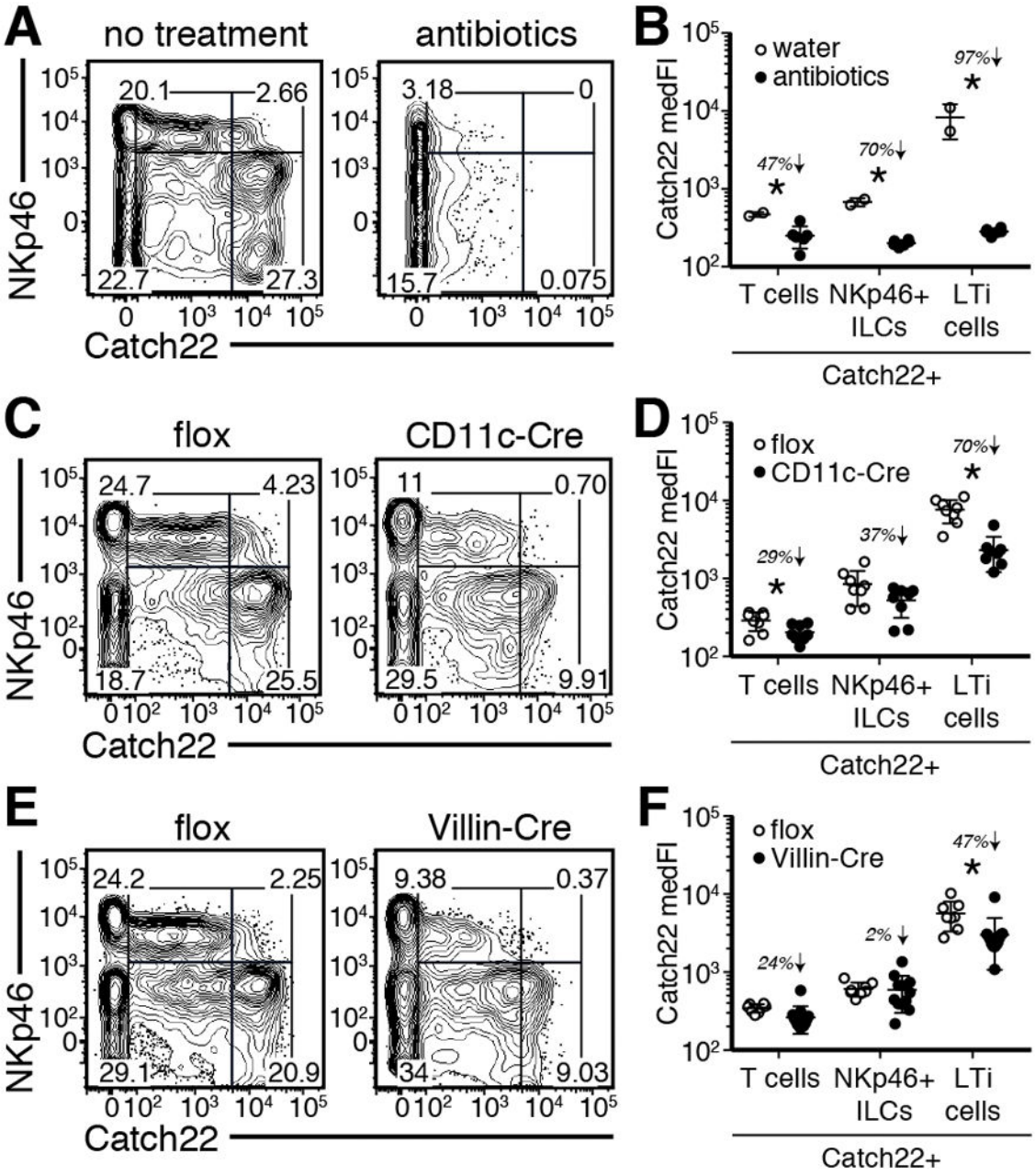

Figure 3.

Microbial sensing drives homeostatic *Il22* activity. (**A,B**) *Il22*$^{C22/+}$ mice were treated with an antibiotic cocktail from embryonic day 12–14 until analysis for Catch22 at post-natal day 29. (n=2 or 6 mice). (**C,D**) Lamina propria from *Il22*$^{C22/+}$;*CD11c-Cre;MyD88*$^{flox/flox}$ mice were analyzed for Catch22^{+} populations at 4.5–7 weeks-old (n=8 each). (**E,F**) Lamina propria from *Il22*$^{C22/+}$;*Villin-Cre;MyD88*$^{flox/flox}$ mice were analyzed for Catch22^{+} populations at 4–5 weeks-old (n=8 or 13). (**A,C,E**) Representative flow plots of ILC (Thy1^{+} CD3^{-}) populations. (**B,D,F**) Median fluorescent intensity of Catch22 in the indicated populations; italicized percentages indicate the reduction in Catch22 MFI relative to

untreated or Cre-negative mice. Significance calculated with Holm-Sidak multiple comparisons correction.

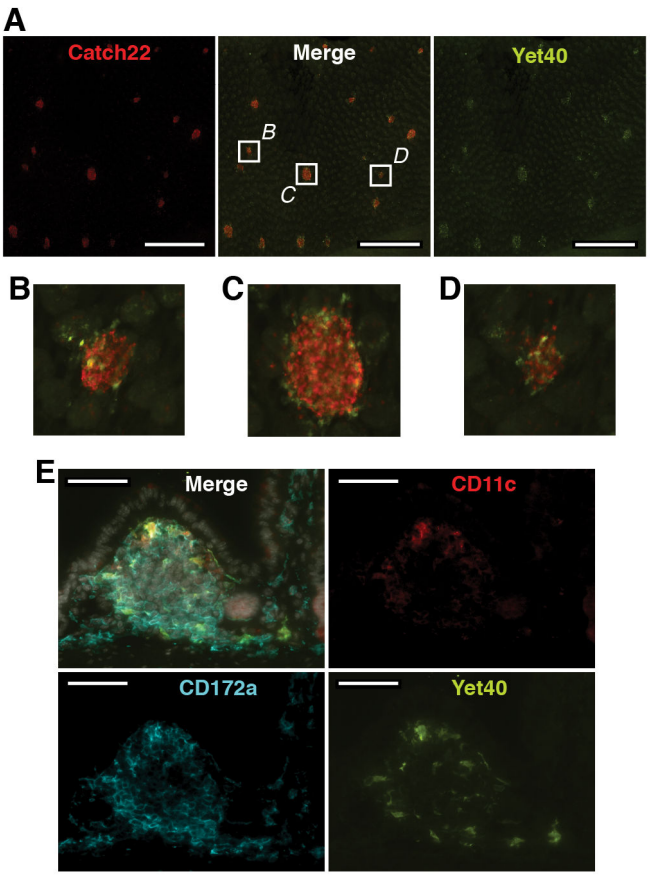

Figure 4.

Il12b^{+} cells are also resident at cryptopatches. (**A**) *Il22*$^{C22/+}$;*Il12b*$^{Y40/+}$ or *Il22*$^{C22/+}$;*Il12b*$^{Y40/Y40}$ murine small intestine was fixed and stained by whole mount for Catch22 (red) and Yet40 (green) (representative of n=4). Scale bar represents 1 mm. (**B–D**) Details of the indicated regions from ***A***. (**E**) Small intestine from *Il12b*$^{Y40/+}$ mice was fixed, sectioned, and stained for Yet40 (green), CD11c (red), CD172a (light blue), and DAPI (gray) (representative of n=6). Scale bar represents 100 μm.

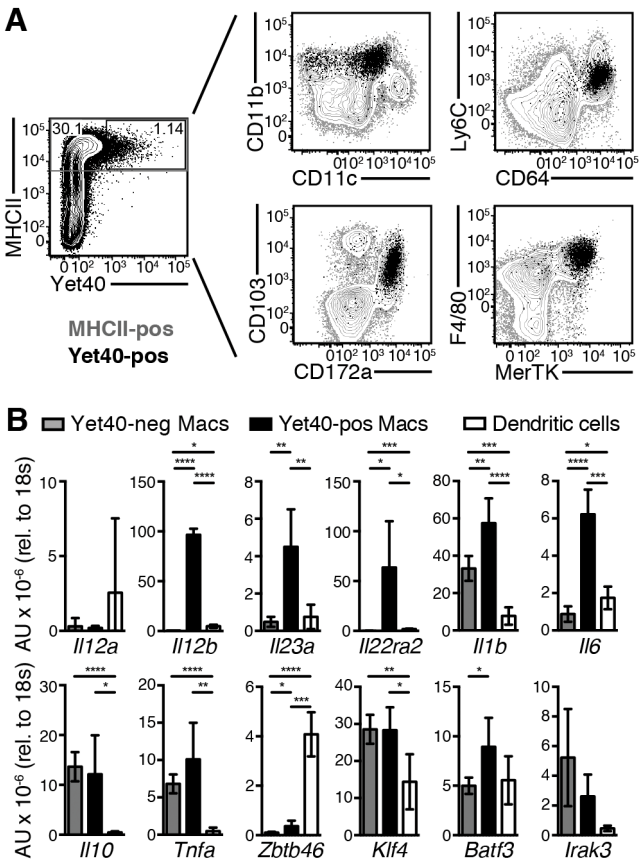

Figure 5.

Yet40^{+} cells are macrophages. (**A**) Lamina propria from *Il12b*$^{Y40/Y40}$ mice was analyzed for Yet40 expression and the indicated markers. The Yet40^{+} gate was set based on a wild-type genetic control (representative of n=6). (**B**) CD45^{+}MHCII^{+} cells from small intestine lamina propria were sorted as Yet40^{+} macrophages ("Yet40-pos Macs": CD11c^{int} CD64^{+} Yet40^{+}), Yet40^{-} macrophages ("Yet40-neg Macs": CD11c^{int} CD64^{+} Yet40^{-}), and dendritic cells (CD11c^{+} CD64^{-}). RNA/cDNA was prepared and analyzed for transcript levels (n=5).

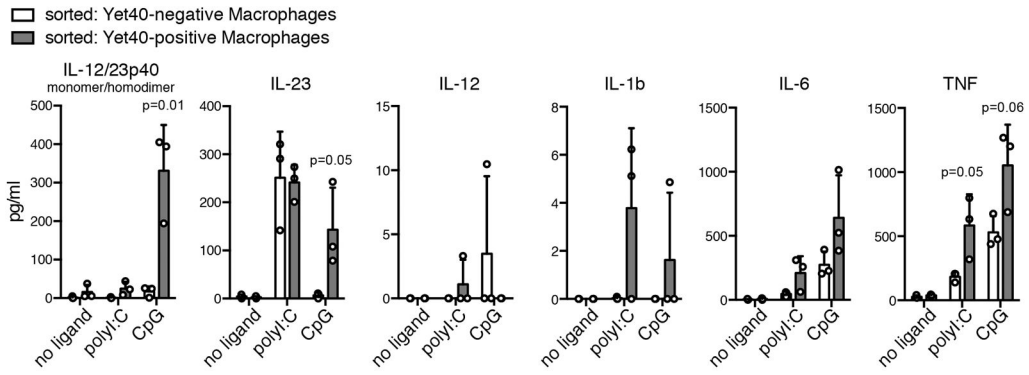

Figure 6.

Yet40^{+} macrophages are more responsive to TLR stimulation. APCs were sorted from *Il12b*$^{Y40/Y40}$ mice and plated overnight in GM-CSF or GM-CSF with TLR3 (poly(I:C)) or TLR9 (CpG) ligand. Culture supernatants were analyzed for the indicated cytokines by cytometric bead array. IL-12/23 p40, IL-23 p19/p40, and IL-12 p35/p40 detections are not cross-reactive, per the manufacturer, such that IL-12/23 p40 signal must represent p40 monomers or homodimers (n=3 from pools of 5–6 mice each). P values calculated for Yet40^{+} vs. Yet40^{-} macrophages for each treatment.

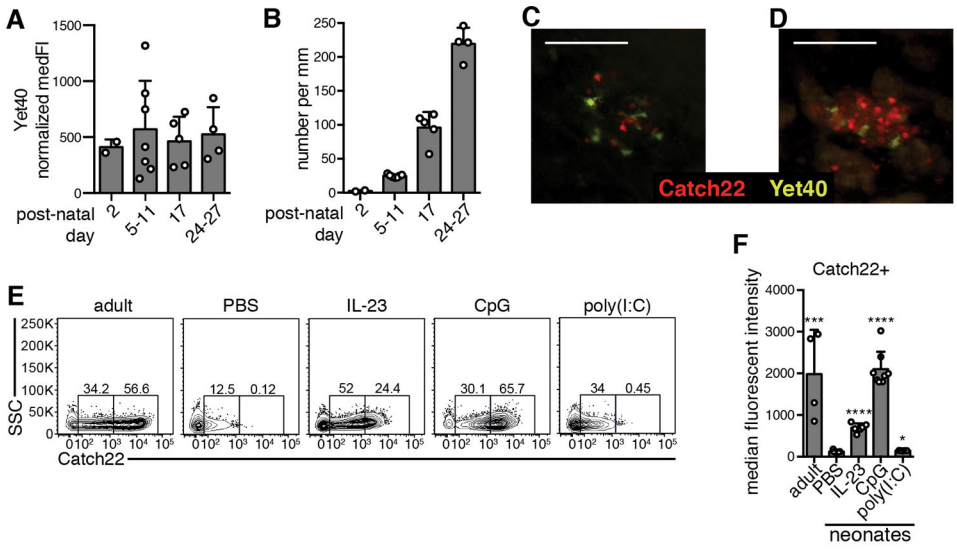

Figure 7.

Yet40^{+} macrophages are present and capable of inducing Catch22 prior to weaning. (**A**,**B**) *Il12b*$^{Y40/Y40}$ murine small intestine was analyzed for Yet40^{+} cells by flow cytometry, for Yet40 MFI among Yet40^{+} cells, normalized to a reporter-negative control (**A**) and total number of Yet40^{+} cells (**B**). Peyer's patches were not removed from 2, 5, or 7 day-old mice (n=2–11 per group). (**C,D**) Small intestine from 11 (**C**) or 17 (**D**) day-old *Il22*$^{C22/+}$;*Il12b*$^{Y40/Y40}$ mice was fixed and stained by whole mount for Catch22 (red) and Yet40 (green) (representative of n=2 per time point). Scale bar represents 100 μm. (**E,F**) 12–14 day-old *Il22*$^{C22/+}$;*Il12b*$^{Y40/Y40}$ mice were injected i.p. with PBS, 2.5 μg IL-23, 100 μg CpG, or 100 μg poly(I:C) on two consecutive days and analyzed on the third day for Catch22 MFI. Adults were untreated (n=4–9 per group). Representative flow plots of LTi cells (**E**) and median fluorescent intensity of Catch22 in Catch22^{+} LTi cells (**F**). t test significance vs. neonatal PBS-treated: * < 0.05, *** < 0.001, **** < 0.0001.